



Research Article

ISSN : 0975-7384  
CODEN(USA) : JCPRC5

## Thermogravimetric and structural studies of zinc-doped magnetite nanoparticles for pharmaceutical application

Irina Vedernikova\*, Alla Koval and Alina Fataliyva

National University of Pharmacy, Inorganic Chemistry Department, 53, Pushkinskaya str., Kharkov, 61002 Ukraine

### ABSTRACT

*In this paper  $Zn_{0.4}Fe_{2.6}O_4$  nanoparticles have been prepared by co-precipitation method. Ferrite nanoparticles are characterized by thermogravimetric and differential thermal analysis (TG-DTA). The crystalline structure of the zinc-doped magnetite nanoparticles have been studied with a help of X-ray diffraction (XRD). The samples show cubic inverse spinel structure with rang size of 9 to 26 nm.*

**Keywords:** Nanoparticles; Co-precipitation; Zinc -Iron oxide.

### INTRODUCTION

Nanoscience is one of the most important research and development frontiers in modern science. One of the most promising of nanomaterials is the ferrite nanoparticles of different compositions. Ferrite nanoparticles offer exciting opportunities in fundamental study and technological applications, such as biomedical applications, bio processing and catalysts, and others [1-5].

Doping magnetite with transition metal elements (zinc, copper, manganese) allows the modification of important quantities as saturation magnetization, optical properties, electroconductivity [6-8]. Zinc belongs to a class of microelements that are considered to play an important role in many vital biochemical reactions and physiological processes: growth and development of the cells, stimulation the gene transcription and cell proliferation, activation of DNA and RNA polymerases, slowdown the oxidation processes, optimization of the human immune system [9-16].

Therefore, to get more information about zinc ferrite nanoparticles and to improve their applications or develop new ones, are essential careful studies related to their stability, functionality, particle sizes and also their materials and physical behaviours. In this work, zinc-doped magnetite nanoparticles are synthesized by co-precipitation method. Ferrite nanoparticles are characterized by thermogravimetric and differential thermal analysis (TG-DTA). The crystalline structure of the zinc-doped magnetite nanoparticles have been with a help studied of X-ray diffraction (XRD).

### EXPERIMENTAL SECTION

#### 2.1. Preparation of zinc-doped magnetite nanoparticles

Ultrafine particles of  $Zn_{0.4}Fe_{2.6}O_4$  have been prepared by coprecipitating aqueous solutions of  $FeSO_4$ ,  $Zn(CH_3COO)_2$  and  $FeCl_3$  mixtures in an alkaline medium (0.1 M NaOH). The reaction mixtures have been maintained at 85 - 90°C for 4 hrs. This time it has been sufficient for the transformation of hydroxides into spinel ferrite. Magnetic particles have been collected using magnetic separation. These particles have been washed several times with distilled water and dried at room temperature, producing thus samples ZMN. Samples ZMN have been heated at 40°C, 500°C and 800°C for 2 h, resulting samples ZMN40, ZMN500 and ZMN800.

## 2.2. Characterization techniques

Simultaneous thermogravimetric and differential thermal analysis (TG–DTA) traces have been obtained from Q-1500D instruments (MOM, Hungary) at a heating rate of 10°C/min.

The X-ray diffraction (XRD) patterns of the samples have been recorded on a Siemens D500 X-ray powder diffractometer using copper radiation. Slow scans of the selected diffraction peaks have been carried out in the step mode (step size 0.03°, measurement time 75 s. The crystallite size of the nanocrystalline samples has been measured from the X-ray line broadening using the Debye-Scherrer formula after accounting for instrumental broadening.

## RESULTS AND DISCUSSION

Firstly, the thermal behavior of the zinc-doped magnetite nanoparticles (ZMN) have been studied by thermal analysis. Figure 1 shows TG, DTG, and DTA curves recorded for  $Zn_{0.4}Fe_{2.6}O_4$  at a constant heating rate of 10°C min<sup>-1</sup> in the temperature range of 20°C to 800°C.

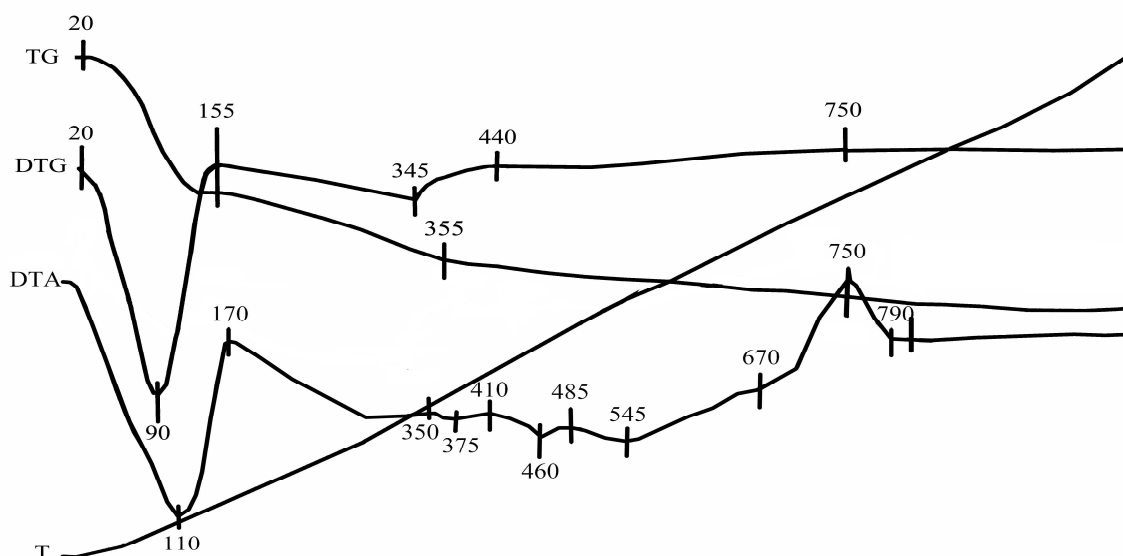


Fig. 1. TG, DTG, and DTA curves of  $Zn_{0.4}Fe_{2.6}O_4$

The TG and DTG curves show that the decomposition of the compounds proceeds in three stages. The first stage that occurred at about 180°C shows 2.5 % weight loss caused by the loss of physical adsorbed water.

In the second stage, an extensive weight loss (1.3%) is observed at about 355°C. The third stage (at about 800°C) shows 0.6 % weight loss. These can be caused by the loss of chemical adsorbed water.

At a temperature of 750 ° C on the curve DTA exothermic peak which corresponds to the synthesis phase of  $ZnFe_2O_4$ . In the temperature range 350 - 545 ° C there is a series of peaks of low intensity exact position and interpretation which is quite complicated.

The XRD pattern for zinc-doped magnetite nanoparticles of samples ZMN40, ZMN500 and ZMN800 are shown Figure 2.

XRD can be used to characterize the crystallinity of nanoparticles, and it gives average diameters of all the nanoparticles. The precipitated fine particles have been characterized by XRD for structural determination and estimation of crystallite size. XRD patterns have been analyzed and indexed using powder X software. All experimental peaks have been matched with the theoretically generated one and indexed. The lattice constant ( $a_0$ ) have been computed. The values of lattice constants for present composites are given in table 1.

Analysis of the diffraction pattern confirms the formation of cubic spinel structure for all the samples. The sample ZMN40 has single phase, the observed lines correspond the standard JCPDS file no. 22-1012 ( $ZnFe_2O_4$ ), there is no appreciable line broadening or detectable sign of any other crystalline or amorphous phase. This result indicates that  $Zn^{2+}$  can be incorporated into  $Fe_3O_4$  lattice with no second phase. In the structure of ZMN500 and ZMN800 phase of  $\alpha$  modification  $Fe_2O_3$  (hematite, the standard JCPDS file no. 33-664) has been analyzed.

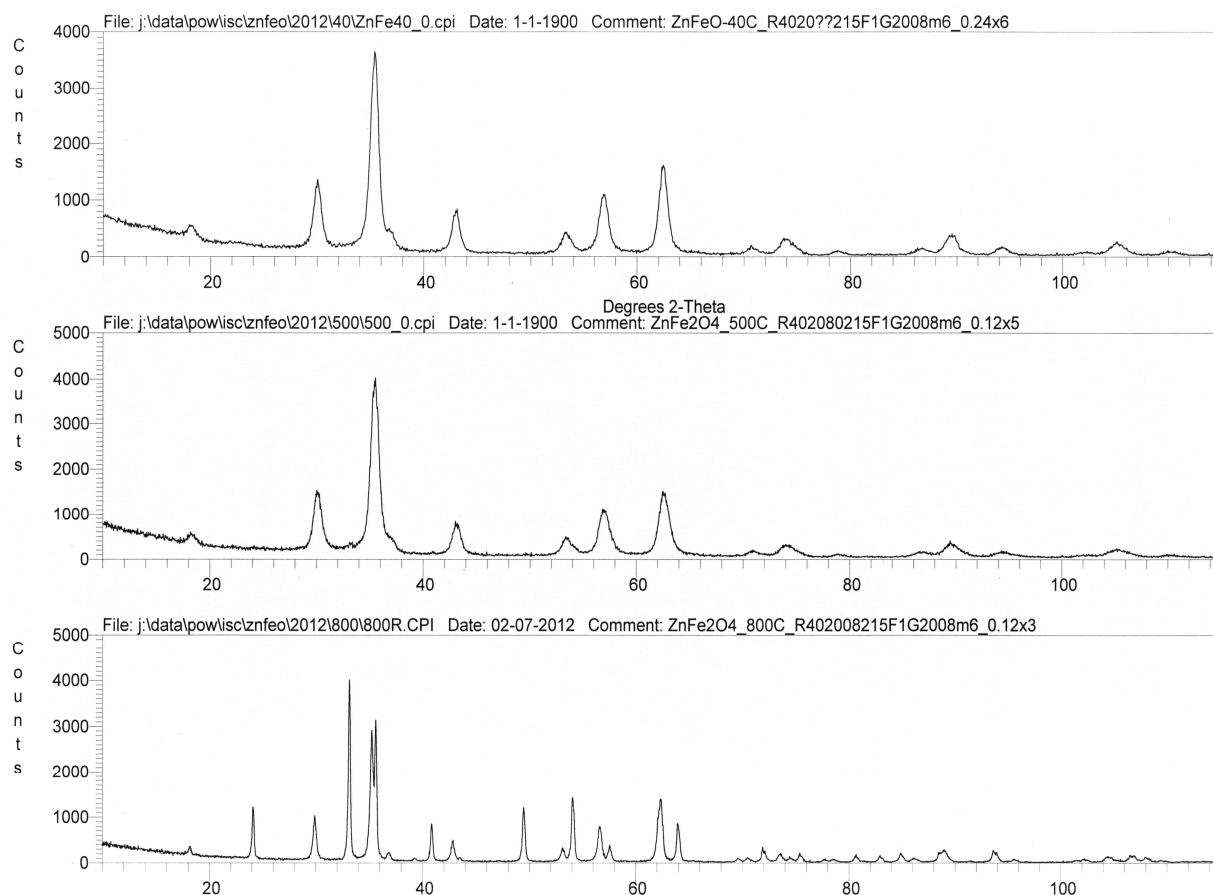


Fig. 2. X-ray diffraction pattern of the ZMN40, ZMN500 and ZMN800 samples (Cu K $\alpha$ ).

Table 1: Phase composition and characteristics of the experimental samples

Sample	Phase	Mass, %	a, (Å)	V, Å <sup>3</sup>	Crystallite size and microstrain, nm/ %
ZNM40	ZnFe <sub>2</sub> O <sub>4</sub>	100(1)	a=8.4060(3)	593.96(4)	9/0.17
ZNM500	ZnFe <sub>2</sub> O <sub>4</sub>	93.9(1.0)	a=8.3960(4)	591.84(4)	10/0.60
	α-Fe <sub>2</sub> O <sub>3</sub>	6.1(6)	a= 5.025(3) c= 13.750(10)	300.6(4)	6/0.06
ZNM800	ZnFe <sub>2</sub> O <sub>4</sub>	39.7(4)	a=8.43724(13)	600.622(16)	26/0.09
	γ-Fe <sub>2</sub> O <sub>3</sub>	60.3(4)	a=5.03473(7) c=13.7450(3)	301.736(8)	103/0.06

Lattice parameters for the spinel phase close to the parameter values for pure magnetite (8.39Å). This may be ascribed to the fact of significant lack of zinc cation in the sample Zn<sub>0.4</sub>Fe<sub>2.6</sub>O<sub>4</sub> compared to formula ZnFe<sub>2</sub>O<sub>4</sub>.

With increasing temperature, sample processing, spinel phase starts to break down. Hematite is formed as a separate phase, while in the spinel structure of ZMN500 there is a noticeable microstrain. A significant decrease in the lattice parameter of spinel in sample ZMN500 in comparison with the sample ZMN40 suggests that the cause of microstrain are oxygen vacancies in the structure. Upon further heating to 800°C (sample ZMN800) the proportion of hematite phase significantly increased, and the composition of spinel phase close to the theoretical, as evidenced by the values of lattice parameter.

For samples, as temperature increases, the mean crystallite diameter progressively increases and the microstrain decreases significantly for ZMN800. The spinel lattice cell parameter has been observed to slightly increase for ZMN800 sample.

Magnetite or Fe<sub>3</sub>O<sub>4</sub> is one of inverse spinel group members with the general formula AB<sub>2</sub>O<sub>4</sub>. In its structure A is Fe<sup>+2</sup> ion and B is Fe<sup>+3</sup> ion. The structure of magnetite consists of closed-packed oxygen arrangement with the divalent Fe<sup>+2</sup> ion in tetrahedral sites and the trivalent Fe<sup>+3</sup> ion in octahedral sites. For ZnFe<sub>2</sub>O<sub>4</sub>, Zn<sup>2+</sup> and Fe<sup>3+</sup>

distribution at A and B sites within the structure can be represented by the formula  $Zn^{2+}_{\delta}Fe^{3+}_{1-\delta}[Zn^{2+}_{1-\delta}Fe^{3+}_{1+\delta}]O_4$ , where  $\delta$  is the inversion parameter.

Further the specification of the Zn cation distribution in samples has been carried out. It is found that the sample ZMN40 in tetrahedral positions has 40% zinc and 60% iron. ZMN500 – tetrahedral positions 61% zinc 39% iron, ZMN800 – 81% and 19% respectively. Octahedral positions in the all samples occupied only by iron. Occupancy of oxygen positions can not be clarified, as well by this method as the valence of iron in different positions.

Thus, the structural formula of spinel in the sample ZMN40 is  $Zn_{0.4}Fe_{0.6}Fe_2O_{4-x}$ , ZMN500 –  $Zn_{0.61}Fe_{0.39}Fe_2O_{4-x}$ , ZMN800 –  $(Zn_{0.81}Fe_{0.19})Fe_2O_{4-x}$ .

### CONCLUSION

For improving structural properties of zinc doping magnetite has been studied. XRD pattern of nanoparticles indicated formation of zinc doping magnetite with cubic inverse spinel structure in all samples. Increasing temperature caused to increasing mean crystallite diameter and formation of hematite phase.

### REFERENCES

- [1] D. Emerich, C. Thanos, *J. Drug Target.*, **2007**, 15, №3, 163–171.
- [2] V. Koppiseti, B. Sahiti, *J. Drug Dev. & Res.*, **2011**, 3, №1, 260–266.
- [3] K. Krishnan, *IEEE Transactions on magnetic*, **2010**, 46, №7, 2523–2558.
- [4] C. Kumar, Darmstadt, Germany: *Wiley VCH*, **2009**, 143
- [5] I. Vizirianakis, *Nanomedicine*, **2011**, №7, 11–17.
- [6] P. Puspitasari, N. Yahya, N. Zabidi, N. Ahmad, *J. Applied Sci.*, **2011**, 11, №7, 1199–1205.
- [7] D. Yener, H. Giesche, *J. Am. Ceram. Soc.*, **2001**, 84, № 9, 1987–1995.
- [8] S. Singhal, T. Namgyal, S. Bansal, K. Chandra, *J. Electromagnetic Analysis & Applications*, **2010**, № 2, 376–381.
- [9] W. Opoka, D. Adamek, M. Plonka, W. Reczynski, B. Bas, D. Drozdowicz, P. Jagielski, Z. Sliwowski, P. Adamski, T. Brzozowski, *Journal Of Physiology And Pharmacology.* – **2010**, 61, № 5, 581–591.
- [10] Lansdown AB, Path RF, Mirastschijski U, et al., *Wound Rep Reg*, **2007**, 15, 2-16.
- [11] Rink L, Haase H., *Trends Immunol*, **2006**, 28, 1-4.
- [12] Schwartz JR, Marsh RG, Draelos ZD., *Dermatol Surg*, **2005**, 31, 837-847.
- [13] Overbeck S, Rink L, Haase H., *Arch Immunol Ther Exp*, **2008**, 56, 15-30.
- [14] Kehl-Fie TE, Skaar EP., *Curr Opin Chem Biol*, **2010**, 14, 218-224.
- [15] Powell SR., *J Nutr*, **2000**, 130, 1447S-1454S.
- [16] Keen CL, Gershwin ME., *Ann Rev Nutr*, **1994**, 10, 415